CDF/PUB/BOTTOM/PUBLIC/10424

First Search for T-violating Triple Products Asymmetries in $B_s^0 \to \phi\phi$ Decays

The CDF Collaboration
URL http://www-cdf.fnal.gov
(Dated: April 7, 2011)

We present the first analysis of Triple Products (TP's) in the $B_s^0 \to \phi\phi$ decay. This uses Tevatron data collected by the upgraded Collider Detector at Fermilab (CDF II) in the period starting from March 2001 till April 2008, which correspond to an integrated luminosity of 2.9 fb^{-1}. Using approximately 300 untagged $B_s^0 \to \phi\phi$ decays, we measure the asymmetries of two functions of the helicity angles:

$$A_u = -0.007 \pm 0.064(\text{stat.}) \pm 0.018(\text{syst.}),$$
$$A_v = -0.120 \pm 0.064(\text{stat.}) \pm 0.016(\text{syst.}).$$

which constrain the TP's asymmetries of this decay mode.

I. INTRODUCTION

The angular analysis of penguin-mediated B meson decays into two vector mesons, as $B_s^0 \to \phi\phi$, can provide evidence for physics beyond Standard Model(SM). The time-integrated angular analysis has been first performed by CDF and allows the measurement of the CP-averaged decay amplitudes of the three helicity states [1]. The amplitudes, given in terms of one longitudinal (A_0) and two transverse ($A_\parallel$ and $A_\perp$) *polarization* amplitudes, result in a dominant transverse polarized fraction in disagreement with the naïve SM expectation. Explanation involving either New Physics (NP) [2, 3] or corrections to naive expectation within the SM, either through penguin annihilation [4–6] or final state interactions [7–10], have been proposed.

Present statistics of the $B_s^0 \to \phi\phi$ data sample does not allow investigations of mixing induced CP-violation. However, a class of CP-violating observables which can reveal the presence of NP are the Triple Products asymmetries [11]. Triple Products (TP) take the form $\vec{p}\cdot(\vec{\varepsilon}_1 \times \vec{\varepsilon}_2)$, where $\vec{p}$ is a momentum and both $\vec{\varepsilon}_i$ can be either spins or momenta. Triple products are odd under time reversal (T), therefore they are sensitive to CP violation assuming CPT invariance. The TP's asymmetry is defined as:

$$\mathcal{A}_{\rm TP} = \frac{\Gamma(\vec{p}\cdot(\vec{\varepsilon}_1 \times \vec{\varepsilon}_2) > 0) - \Gamma(\vec{p}\cdot(\vec{\varepsilon}_1 \times \vec{\varepsilon}_2) < 0)}{\Gamma(\vec{p}\cdot(\vec{\varepsilon}_1 \times \vec{\varepsilon}_2) > 0) + \Gamma(\vec{p}\cdot(\vec{\varepsilon}_1 \times \vec{\varepsilon}_2) < 0)}, \tag{1}$$

where Γ is the decay rate for the given process. Most of these TP's asymmetries are expected to be small in the SM, but can be enhanced in the presence of NP [12].

We report the first investigation on TP's asymmetries of the $B_s^0 \to \phi\phi$ decay, reconstructed from the detection of the charged kaon pairs from the ϕ's, $B_s^0 \to \phi\phi \to [K^+K^-][K^+K^-]$, in the same data sample used for the polarization amplitudes measurement [1]. This correspond to an integrated luminosity of 2.9 fb^{-1}, where about 300 $B_s^0 \to \phi\phi$ decays are reconstructed. Without tagging initial flavor of the B_s^0 mesons the decay rate is just the sum of the B_s^0 and the $\bar{B}_s^0$ one, produced in equal proportion at Tevatron. In the untagged case the TP's asymmetries are proportional to the so called *true* Triple Products, that is a true CP violating effect. The so called *fake* Triple Products are not accessible instead in the untagged case and are not discussed here [11, 12].

II. $\mathcal{A}_{\rm TP}$'S IN $B_s^0 \to \phi\phi$

In the $B_s^0 \to \phi\phi$ decay two TP's exist, given by the interference terms of the CP even and CP odd decay amplitudes. The first, TP_1, is $\Im(A_\parallel A_\perp^\star)$; the second, TP_2, is $\Im(A_0 A_\perp^\star)$.

The differential decay rate for the $B_s^0 \to \phi\phi \to [K^+K^-][K^+K^-]$ decay chain as function of the helicity angles is fully described in ref [1]. The definition of the helicity angles $\vec{\omega} = (\cos\vartheta_1, \cos\vartheta_2, \Phi)$ is shown graphically in fig. 1.

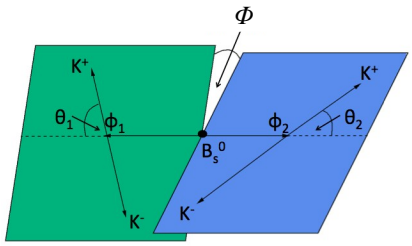

FIG. 1: Sketch of the helicity angles. Defining the direction of momentum of the ϕ_i $(i = 1, 2)$ in the B rest frame as $\hat{q}_i$, ϑ_i is the angle between $\hat{q}_i$ and the momentum of the K_i^+, defined in the rest frame of the ϕ_i; the Φ angle is the angle between the decay planes of the ϕ's.

The decay rate as a function of time and the helicity angles can be written as

$$\frac{d^4\Lambda(\vec{\omega}, t)}{dt\, d\vec{\omega}} = \frac{9}{32\pi} \sum_{i=1}^{6} K_i(t) f_i(\vec{\omega}), \tag{2}$$

where the angular functions $f_i(\vec{\omega})$ are given by

$$\begin{aligned} f_1(\vec{\omega}) &= 4\cos^2\vartheta_1\cos^2\vartheta_2, \\ f_2(\vec{\omega}) &= \sin^2\vartheta_1\sin^2\vartheta_2(1+\cos 2\Phi), \\ f_3(\vec{\omega}) &= \sin^2\vartheta_1\sin^2\vartheta_2(1-\cos 2\Phi), \\ f_4(\vec{\omega}) &= -2\sin^2\vartheta_1\sin^2\vartheta_2\sin 2\Phi, \\ f_5(\vec{\omega}) &= \sqrt{2}\sin 2\vartheta_1\sin 2\vartheta_2\cos\Phi, \\ f_6(\vec{\omega}) &= -\sqrt{2}\sin 2\vartheta_1\sin 2\vartheta_2\sin\Phi, \end{aligned} \tag{3}$$

while the functions $K_i(t)$ encode the B_s^0 time evolution including mixing and depend on the polarization amplitudes. In particular K_4 and K_6 terms are proportional to the measured quantities TP_1 and TP_2. In the SM, where only one weak phase is involved in the decay, and with an almost vanishing B_s^0 mixing phase the K_4 and K_6 terms vanish in the untagged rate for any value of t. In the presence of NP in the decay or in the mixing one can instead expect a non zero value for K_4 and K_6 terms.

We can access TP_1 through the observable $u = \cos\Phi\sin\Phi$. We define the u asymmetry from the sample with positive and negative value of u:

$$A_u = \frac{N^+ - N^-}{N^+ + N^-}, \tag{4}$$

where N^+ (N^-) is the number of events with $u > 0$ ($u < 0$). This asymmetry is proportional to $\mathcal{A}_{\mathrm{TP}_1}$but is also sensitive to mixing induced Triple Products when considering the decay width difference of the B_s^0 system mass eigenstates.

The TP_2 asymmetry is similarly accessed looking at $v = \sin\Phi$ in bins of $\cos\vartheta_1\cos\vartheta_2$, and defining an asymmetry of its distribution:

$$A_v = \frac{M^+ - M^-}{M^+ + M^-}, \tag{5}$$

where M^+ (M^-) is the number of events with $v > 0$ ($v < 0$) depending on the $\cos\vartheta_1\cos\vartheta_2$ bin. As before this asymmetry is proportional to $\mathcal{A}_{\mathrm{TP}_2}$but is also sensitive to mixing induced Triple Products when considering the decay width difference of the B_s^0 system mass eigenstates.

III. DETECTOR TRIGGER AND DATA SAMPLE

The CDF II detector is described in detail elsewhere [13]. Most relevant to this analysis are the tracking and trigger systems. Three-dimensional charged particle tracking is achieved through an integrated system consisting of 6 layers of double-sided silicon detectors between 2.5 and 10 cm and 96 samplings in a large drift chamber (COT) [14] between 30 and 132 cm, all contained in a superconducting solenoid generating 1.41 T magnetic field.

Hadronic B decays are collected via a dedicated track trigger capable of identifying tracks displaced from the primary vertex due to the long lifetime of b-hadrons. The online track reconstruction is performed at first level trigger in the COT by the XFT track processor [15] and by the Silicon Vertex Tracker (SVT) [16] at the second level. The latter combines the XFT and silicon detector informations achieving an impact parameter resolution comparable with the offline one.

The analysis described here uses a data sample selected requiring two charged tracks with transverse momenta $p_{\mathrm{T}} \geq 2$ GeV/c and with impact parameter 120 μm $\leq d_0 \leq$ 1000 μm. Furthermore the two trigger tracks must have an opening angle in the transverse plane satisfying $2^\circ \leq |\Delta\phi| \leq 90^\circ$ and $L_{xy} \geq 200$ μm, where the two dimensional decay length, L_{xy}, is calculated as the transverse distance from the beam line to the two track vertex projected along the total transverse momentum of the track pair.

The sample has been collected in the data taking period from the beginning of Run II till April 2008, and the integrated luminosity is 2.9 ± 0.2 fb^{-1}. We reconstruct the two body B_s^0 decay to two $\phi(1020)$ vector mesons with $\phi(1020) \to K^+K^-$ (BR=(49.2 ± 0.6)% [17]), the final states thus consists of 4 charged kaons emerging from a single displaced vertex. To reconstruct B_s^0 candidate all four-track combinations that satisfy trigger criteria are fit to a common vertex. All the tracks that are used in the vertex fit are required to have both drift chamber and silicon vertex hits and a minimum transverse momentum of 400 MeV/c. Opposite charge track pairs with invariant mass within 15 MeV/c^2 from the $\phi(1020)$ mass PDG value [17] are considered $\phi(1020)$ candidates.

L^B_{xy}	> 330 μm
$p^K_{\mathrm{T\,min}}$	> 0.7 GeV/c
χ^2_{xy}	< 17
d^B_0	< 65 μm
$d^{\phi_{\max}}_0$	> 85 μm

TABLE I: Optimized selection cuts.

IV. OPTIMIZATION PROCEDURE

Large backgrounds due to random track combinations and to ϕ production from heavy flavor decays combined with two other random tracks need to be reduced in order to identify the $B^0_s \to \phi\phi$ signals. We inherit the set of cuts on discriminating variables from the BR an polarization analysis [1, 18]. We report here only the resulting selection requirements (TAB. I) on the following kinematic variables of the $B^0_s \to \phi\phi$ decay:

- L^B_{xy}: transverse decay length of the reconstructed B;
- d^B_0: impact parameter of the reconstructed B;
- $d^{\phi_{\max}}_0$: impact parameter of the ϕ with higher momentum;
- $p^K_{\mathrm{T\,min}}$: transverse momentum of the softer kaon;
- χ^2_{xy}: χ^2 of the fit used in the reconstruction of the secondary vertex.

V. THE DATA SAMPLE

Applying the cuts listed in TAB. I, the invariant mass distribution $m_{K^+K^-K^+K^-}$ is obtained (FIG. 2). We identify at least three components:

the signal: it appear as a narrow mass peak whose width is dominated by experimental resolution and whose yield is 295 ± 20 events.

combinatorial background: these are random combinations of charged tracks accidentally satisfying the selection requirements. They produce a smooth slowly-decreasing distribution. This is the more important source of background.

physics background: it is due to partially reconstructed or mis-reconstructed (*reflections*) B-hadron decays. We expect a distribution peaking near the signal for several decays: $B^0 \to \phi K^\star \to [K^+K^-][K^+\pi^-]$ and $B^0_s \to \bar{K}^\star K^\star \to [K^+\pi^-][K^+\pi^-]$; these reflections occur when the $K^\star$ is incorrectly reconstructed as a ϕ. The estimated number of reflection events is [18]:

	$B^0_s \to K^\star K^\star$	$B^0 \to \phi K^\star$
Events	0	8 ± 3
Fraction relative to the signal [%]	10^{-6}	3 ± 1

The $B^0 \to \bar{K}^\star K^\star$ reflection will be neglected in the following due to the smallness of its expected contribution.

Including a possible background asymmetry, a first raw count for u and v distributions gives: $N^+ = 169$, $N^- = 169$ and $M^+ = 153$, $M^- = 185$, therefore, $A_u = (0.0 \pm 5.4)\%$ and $A_v = (-9.5 \pm 5.4)\%$. In fig. 3, the u and the v distributions of those B^0_s candidates in the signal region ([5.319;5.419] GeV/c^2) after side-bands subtraction are shown [19]. No significant asymmetry is evident in the u distribution, while the v distribution is slightly asymettric.

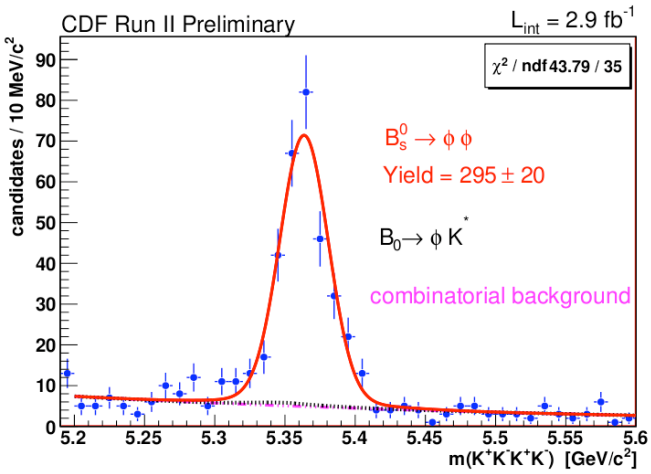

FIG. 2: Mass distributions of the $B_s^0 \to \phi\phi$ decay. The blue points represent data after the optimized selection; the red line is the total fit distribution, the dashed purple line represents the combinatorial background and the black dotted line the small reflection component under the signal peak.

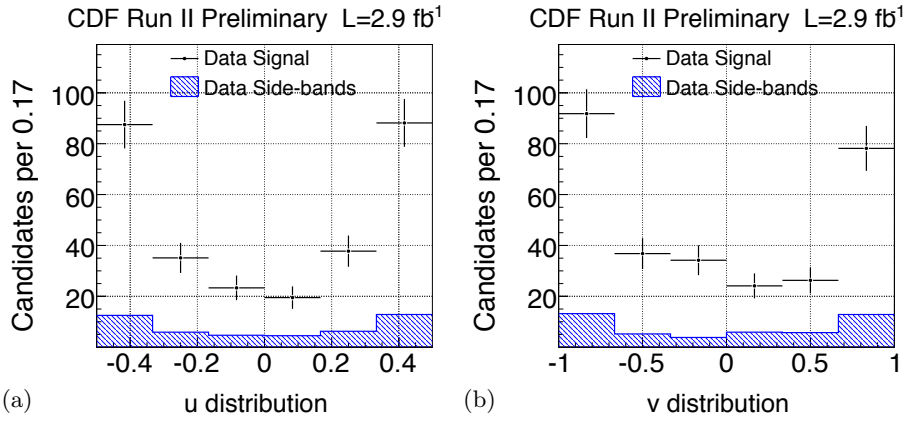

FIG. 3: Distribution of u (a) and v (b) for B_s^0 candidates in the signal region ([5.319;5.419] GeV/c^2). Black points with error bars are sidebands-subtracted data; blue (hatched) histogram represents sideband data.

VI. MEASUREMENT OF THE TRIPLE PRODUCT ASYMMETRIES

The asymmetries A_u and A_v are evaluated through an unbinned Maximum Likelihood fit. First, we consider the N candidates in the range [5.2; 5.6] GeV/c^2 and we split this sample into two subsamples made of N^+ (M^+) and N^- (M^-) events, according to the sign of u (v) of the events. Using large sample of MC data generated with uniform angular distribution, we check that the detector acceptance and the reconstruction requirements are not introducing artificial asymmetries in the u and v distributions. No bias was found with a 0.2% accuracy in the splitting procedure. Then, we fit the invariant mass distribution of each subsets. The fit technique is presented in the following for the u observables, but the same method is applied to the case of v.

Calling N_s^+ and N_s^- the number of signal events in the N^+ and N^- sets respectively, the asymmetry is defined as:

$$A_u = \frac{N_s^+ - N_s^-}{N_s^+ + N_s^-} = \frac{N_s^+ - N_s^-}{N_s}, \tag{6}$$

where $N_s = N_s^+ + N_s^-$ is the number of all signal events. Considering the fractions of signal events in each sample,

f_s^i (where $i = +, -$), and the fraction of signal in the entire sample, f_s, we can write:

$$\begin{aligned} f_s^+ &= f_s \frac{N}{N^+} \frac{1 + A_u}{2} \\ f_s^- &= f_s \frac{N}{N^-} \frac{1 - A_u}{2} \end{aligned} \tag{7}$$

Following the same parameterization in [1], the probability density function (PDF) for each sample is:

$$g^i(m_i|\vec{\xi}) = f_s^i \mathcal{G}(m_i|M, \sigma) + (1 - f_s^i)\mathcal{B}(m_i|\lambda), \tag{8}$$

where $\vec{\xi}$ is the parameters vector, m^i is the mass of a candidate in the sample N^i, and:

- $\mathcal{G}(m_i|M, \sigma)$ is the sum of two gaussian with same mean value M but different resolutions, σ and $k\sigma$, which describes the signal component:

$$\mathcal{G}(m_i|M, \sigma) = h \frac{1}{\sqrt{2\pi}\sigma} e^{-\frac{(m_i - M)^2}{2\sigma^2}} + (1 - h) \frac{1}{\sqrt{2\pi}k\sigma} e^{-\frac{(m_i - M)^2}{2k^2\sigma^2}}, \tag{9}$$

  where h is the fraction of one gaussian component with respect to the other. This choice is fairly standard and takes into account the detector effects that cause an additional spread in the tail distributions. In the final fit the multiplicative factor k and the fraction h are fixed from the fit to large MC data sample, M is fixed to the PDG value of the B_s^0 mass, while σ is left free.

- $\mathcal{B}(m_i|\lambda)$ describes the combinatorial background through an exponential function whose slope, λ, is floating in the fit.

The reflection component is ignored in the fit and and we account for this in the systematic uncertainty (section VII).

The likelihood for each subsample is:

$$\mathcal{L}^i(\vec{m}_i|\vec{\xi}) = \prod_{j=1}^{N^i} g^i(m_{ij}|\vec{\xi}) \tag{10}$$

The fit to the N^+ and N^- samples are performed simultaneously, taking the product of the two likelihood. We must consider fluctuations of N^+ and N^- with the constrain $N = N^+ + N^-$. We treat N^+ and N^- as binomially distribuited, with a probability p to have N^+ events having N total; thus, we multiply the total Likelihood by the binomial PDF $f(N^+, N^-|p)$.

The splitting probability p is a combination of the total signal fraction f_s, the signal asymmetry A_u and a possible background asymmetry A_b:

$$p = \frac{1}{2}(1 + A_u f_s + (1 - f_s)A_b). \tag{11}$$

Finally, the total likelihood is:

$$\mathcal{L}(\vec{m}|\vec{\xi}) = \prod_{j=1}^{N^+} g^+(m_{+j}|\vec{\xi}) \prod_{l=1}^{N^-} g^-(m_{-l}|\vec{\xi}) f(N^+, N^-|\vec{\xi}). \tag{12}$$

where in $g^i(m_{ij}|\vec{\xi})$ we write the fractions f_s^i in terms of A_u, f_s and A_b. Thus, since we assume the parameters σ and λ are the same for the N^+ and N^- sample, the floating parameters in the final fit are the following six:

$$\vec{\xi} = \{A_u, f_s, A_b, \sigma, \lambda\}. \tag{13}$$

The same fit is performed in the estimate of A_v, with the following replacements: $u \to v$, $N^+ \to M^+$, $N^- \to M^-$, $A_u \to A_v$. The fitter was extensively tested and validated using simulated samples with varying input asymmetries and gives unbiased result with correct uncertainty estimates.

A. Fit results

The fit results are reported in tab. II for both asymmetries A_u and A_v, while in tab. III the correlation coefficients of the fitted parameters are shown.

The fit projection on the two subsamples are shown in fig. 4 and fig. 5 for A_u and A_v respectively.

Parameter	Fitted value
A_u	-0.0074 ± 0.0643
A_b	-0.0417 ± 0.0862
f_s	0.616 ± 0.030
σ	0.0174 ± 0.0011
λ	2.68 ± 0.66
ν	486 ± 22

Parameter	Fitted value
A_v	-0.1197 ± 0.0639
A_b	-0.0095 ± 0.0857
f_s	0.615 ± 0.030
σ	0.0174 ± 0.0012
λ	2.68 ± 0.66
ν	486 ± 22

TABLE II: Fit results for the u (left) and v (right) asymmetries.

	A_u	A_b	f_s	σ	λ	ν
A_u	1.000	-0.233	0.041	0.062	0.002	0.000
A_b		1.000	-0.063	-0.085	-0.002	0.000
f_s			1.000	0.355	-0.018	0.000
σ				1.000	-0.020	0.000
λ					1.000	0.000
ν						1.000

	A_v	A_b	f_s	σ	λ	ν
A_v	1.000	-0.227	0.030	0.020	-0.003	0.000
A_b		1.000	0.018	0.018	0.002	0.000
f_s			1.000	0.351	-0.017	0.000
σ				1.000	-0.019	0.000
λ					1.000	0.000
ν						1.000

TABLE III: Correlation coefficients of the fitted parameters for u (upper) and v (lower) asymmetries.

VII. SYSTEMATIC UNCERTAINTIES

Considering the dominant statistical uncertainity of the asymmetry measurement, only main systematic sources are taken into account. The following effects are considered:

- Ignoring reflection background and other possible components from f^0 and non-resonant decays. Due to the small contribution of the B^0 reflection as well as other B_s^0 signal contribution (up to few per cent of the signal yield), these has been disregarded in the likelihood fit. We compute its contribution as a systematic uncertainty by fitting a large set of pseudo-experiments where the expected fraction of background events are all added either to the N^+ (M^+) or to the N^- (M^-) sample. In this way we maximize their effect on the asymmetry measurement.
- Different function parametrizations for the combinatorial background. We study the impact of the specific combinatorial background model used with respect to different parametrizations.

Adding in quadrature the uncertainties of the different systematic sources we obtain for A_u a total systematic uncertainty of 1.8% while for A_v this is 1.6%.

VIII. CONCLUSIONS

We have performed the first search for CP violation in $B_s^0 \to \phi\phi$ decays. This uses the time integrated $B_s^0 \to \phi\phi$ rate in a data sample corresponding to 2.9 fb^{-1}of integrated luminosity. In particular we measure the asymmetries of two functions of the helicity angles:

$$\begin{aligned} A_u &= -0.007 \pm 0.064(\text{stat.}) \pm 0.018(\text{syst.}), \\ A_v &= -0.120 \pm 0.064(\text{stat.}) \pm 0.016(\text{syst.}) \end{aligned} \tag{14}$$

The first asymmetry, A_u, is well consistent with 0 within experimental uncertainties; the second one, A_v, is 1.8 σ from 0 considering both statistical and systematic uncertainties. These asymmetries constrain the size of two T-violating triple products asymmetries of the $B_s^0 \to \phi\phi$, $\mathcal{A}_{\mathrm{TP}_1} = \Im(A_\parallel A_\perp^\star) - \Im(\bar{A}_\parallel \bar{A}_\perp^\star)$ and $\mathcal{A}_{\mathrm{TP}_2} = \Im(A_0 A_\perp^\star) - \Im(\bar{A}_0 \bar{A}_\perp^\star)$, respectively, expected null in the SM.

Acknowledgments

We thank I. Bigi, A. Datta, D. London and J. Rosner for very useful discussions and suggestions in the understanding of the analysis presented. We thank the Fermilab staff and the technical staffs of the participating institutions for their vital contributions. This work was supported by the U.S. Department of Energy and National Science Foundation;

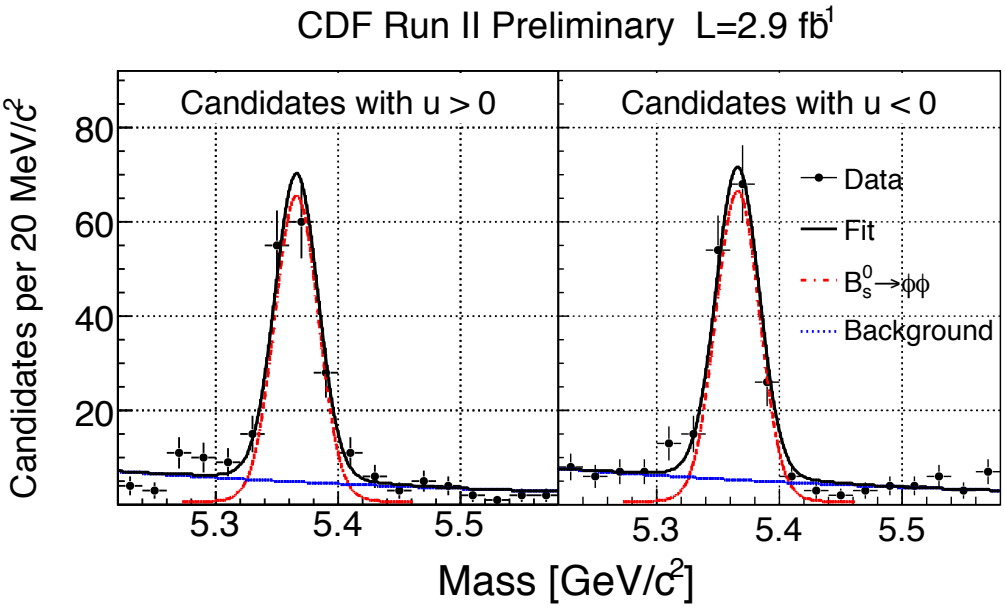

FIG. 4: Fit projections for A_u : N^+ sample (left) and N^- sample (right). The curves shows the fit functions and represent: the $B_s^0 \to \phi\phi$ signal (red), the combinatorial background (dotted blue), and the total projection (black).

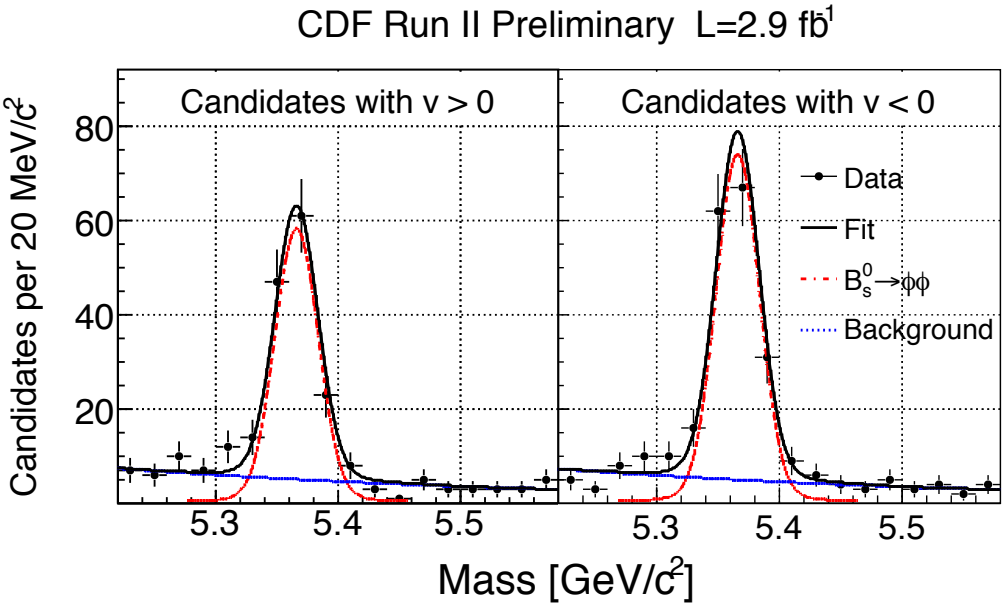

FIG. 5: Fit projections for A_v: M^+ sample (left) and M^- sample (right). The curves shows the fit functions and represent: the $B_s^0 \to \phi\phi$ signal (red), the combinatorial background (dotted blue), and the total projection (black).

the Italian Istituto Nazionale di Fisica Nucleare; the Ministry of Education, Culture, Sports, Science and Technology of Japan; the Natural Sciences and Engineering Research Council of Canada; the National Science Council of the Republic of China; the Swiss National Science Foundation; the A.P. Sloan Foundation; the Bundesministerium für Bildung und Forschung, Germany; the World Class University Program, the National Research Foundation of Korea; the Science and Technology Facilities Council and the Royal Society, UK; the Institut National de Physique Nucleaire et Physique des Particules/CNRS; the Russian Foundation for Basic Research; the Ministerio de Ciencia e Innovación,

and Programa Consolider-Ingenio 2010, Spain; the Slovak R&D Agency; and the Academy of Finland.

---

[1] The CDF collaboration. Measurement of the Polarization Amplitudes of the $B_s^0 \to \phi\phi$ decay. *CDF Pubblic Note*, 10120, 2010.

[2] Ezequiel Alvarez, Luis N. Epele, Daniel Gomez Dumm, and Alejandro Szynkman. Right handed currents and FSI phases in $B^0 \to \phi K^{\star 0}$. *Physical Review D*, 70:115014, 2004.

[3] C. S. Kim and Ya-Dong Yang. Polarization Anomaly in $B \to \phi K^{\star 0}$ and Probe of Tensor Interactions, 2004.

[4] Martin Beneke and Johannes Rohrer and Deshan Yang. Branching fractions, polarisation and asymmetries of $B \to VV$ decays. *Nuclear Physics B*, 774(1-3):64 – 101, 2007.

[5] Ahmed Ali, Gustav Kramer, Ying Li, Cai-Dian Lu, Yue long Shen, Wei Wang, and Yu-Ming Wang. Charmless non-leptonic B_s decays to PP, PV and VV final states in the pQCD approach. *Physical Review D*, 76:074018, 2007.

[6] Alexander L. Kagan. Polarization in $B \to VV$ decays. *Phys. Lett. B*, 601:151–163, 2004.

[7] P. Colangelo, F. De Fazio, and T. N. Pham. The riddle of polarization in $B \to VV$ transitions. *Phys. Lett. B*, 597:291–298, 2004.

[8] Massimo Ladisa, Vincenzo Laporta, Giuseppe Nardulli, and Pietro Santorelli. Final state interactions for $B \to VV$ charmless decays. *Phys. Rev.D*, 70:114025, 2004.

[9] Hai-Yang Cheng, Chun-Khiang Chua, and Amarjit Soni. Final state interactions in hadronic B decays. *Phys. Rev.D*, 71:014030, 2005.

[10] Christian W. Bauer, Dan Pirjol, Ira Z. Rothstein, and Iain W. Stewart. $B \to M(1)M(2)$: Factorization, charming penguins, strong phases, and polarization. *Phys. Rev. D*, 70:054015, 2004.

[11] Alakabha Datta and David London. Triple-Product Correlations in $B \to V_1V_2$ Decays and New Physics. *International Journal of Modern Physics A*, 19:2505, 2004.

[12] Alakabha Datta, Murugeswaran Duraisamy, and David London. Searching for New Physics with B-Decay Fake Triple Products. arXiv:1103.2442, 2011.

[13] R. Blair and others (CDF II Collaboration). The CDF II Detector, Technical Design Report. *FERMILAB-Pub-96/390-E CDF*, 1996.

[14] A. Affolder et al. CDF Central Outer Tracker. *Nucl. Instrum. Methods*, A526, 2004.

[15] E. J. Thomson et al. Online Track Processor for the CDF Upgrade. *IEEE Trans. Nucl. Sci.*, 49, 2002.

[16] B. Ashmanskas et al. The CDF Silicon Vertex Trigger. *Nucl. Instrum. Methods*, A518, 2004.

[17] C. Amsler et al. Particle Data Group. *Physics Letters B*, 667, 2008 and 2009 partial update for the 2010 edition.

[18] The CDF collaboration. Updated Measurement of the $B_s^0 \to \phi\phi$ Branching Ratio Using 2.9 fb^{-1}. *CDF Pubblic Note*, 10064, 2010.

[19] Two side-bands are defined: the left one from 5.2 to 5.3 GeV/c^2 and the right one from 5.43 to 5.6 GeV/c^2